NJC

PAPER

Cite this: *New J. Chem.*, 2018, **42**, 16846

Phosphorescent cyclometalated iridium(III) complexes: synthesis, photophysics, DNA interaction, cellular internalization, and cytotoxic activity†

Satish S. Bhat, *[a] Vidyanand K. Revankar,*[a] Rahul V. Pinjari,[b] S. Naveen,[c] N. K. Lokanath,[d] Vijay Kumbar,[e] Kishore Bhat[e] and Dhoolesh G. Kokare[a]

Received 7th July 2018,
Accepted 11th September 2018

DOI: 10.1039/c8nj03390k

rsc.li/njc

Iridium(III) complexes containing quinoline-appended polypyridyl ligands $[Ir(ppy)_2(qip)]^+$ (**1**) and $[Ir(bhq)_2(qip)]^+$ (**2**) {ppy = 2-phenylpyridine, bhq = benzo[*h*]quinoline, Qip = 2(1*H*)-quinolinone-3(1*H*)-imidazo[4,5*f*][1,10]-phenanthrolin-2-yl} have been synthesized and characterized. The structure of complex **2** has been determined by single crystal X-ray crystallography. The experimental photophysical properties of the complexes have been compared with the theoretically obtained results by density functional theory (DFT) and time-dependent density functional theory (TD-DFT) studies. The HOMO of the complexes is mainly localized on the iridium atom while the LUMO is mainly localized on the proximal position of the N–N donor polypyridyl ligand and the LUMO+1 is localized on the distal portion of the N–N donor polypyridyl ligand. The binding of complexes to double-stranded calf thymus DNA (CT-DNA) has been investigated by absorption and emission spectroscopic techniques. The electrophoretic mobility shift assay of plasmid DNA in the presence of complexes shows DNA aggregation at micro-molar concentration. These complexes have low toxicity and their strong intracellular luminescence highlights their potential as theragnostic agents.

Introduction

Transition metal complexes that interact with DNA have attracted attention from researchers due to their applications such as structure probes, footprinting agents, sequence-specific binding, gene engineering and in drug development.[1–5] These coordination complexes lead to varied series of reactivities/properties due to their variable geometry and coordination number, and different redox, kinetic and thermodynamic properties. Encouraged by the serendipitous discovery and clinical success of the potent anticancer agent *cis*-platin,[6–9] research into transition metal complexes that interact with DNA has flourished.

The luminescent d^6 metal–ion complexes based on ruthenium that bind to DNA through intercalation have been particularly well studied.[10–13] Concurrently, the coordination chemistry of another d^6 transition metal ion Ir^{III} has been rapidly developing. Iridium(III) cyclometalated complexes have been in the spot light due to their photoluminescence color tunability, photo-stability and high quantum yields leading to optical applications such as sensors,[14–18] organic light emitting diodes,[19–25] and biomedical imaging.[26–28] The excellent photo-stability of iridium complexes and their good cell permeability along with high quantum yield make them attractive alternatives to fluorescent organic dyes for bio-imaging and labelling.[29,30] The electronic and steric properties of the iridium(III) complexes can be easily tuned by modifying the ligands leading to a range of geometries useful for providing added chemical planetary about the active sites of enzymes and proteins. In addition to the anticancer activity of iridium complexes, their high photostability, large Stokes shift, and large phosphorescence life time offer better avenues for designing new therapeutic molecules.[31–37] Additionally mixing of C, N-donor ligands with N, N-donor ligands in iridium complexes also leads to better efficacy against cancer cells[36,38–40] by increasing the electron density at the iridium center and making it labile.

[a] *Department of Chemistry, Karnatak University, Dharwad-580003, Karnataka, India. E-mail: bhatsatish111@gmail.com, vkrevankar@rediffmail.com*
[b] *School of Chemical Science, Swami Ramanand Teerth, Marathwada University, Nanded, 431606, Maharashtra, India*
[c] *Department of Physics, School of Engineering and Technology, Jain University, Bangalore 562112, India*
[d] *Department of Studies in Physics, University of Mysore, Manasagangotri, Mysuru 570006, India*
[e] *Maratha Mandal's Central Research Laboratory, Marathamandal Dental College and Research Centre, Belgaum, Karnataka, India*

† Electronic supplementary information (ESI) available: ESI-MS spectra of ligands and complexes, crystallographic data of complex **2**, the bond angle and bond length table (Table S1), the single crystal packing diagram of complex **2**, DFT geometry optimized structures of complexes **1** and **2**, molecular orbital energy diagrams of complexes **1** and **2**, fluorescence microscopy images of DNA condensates, and molecular orbital contributions of complexes **1** and **2** (Table S2). CCDC 1819244. For ESI and crystallographic data in CIF or other electronic format see DOI: 10.1039/c8nj03390k

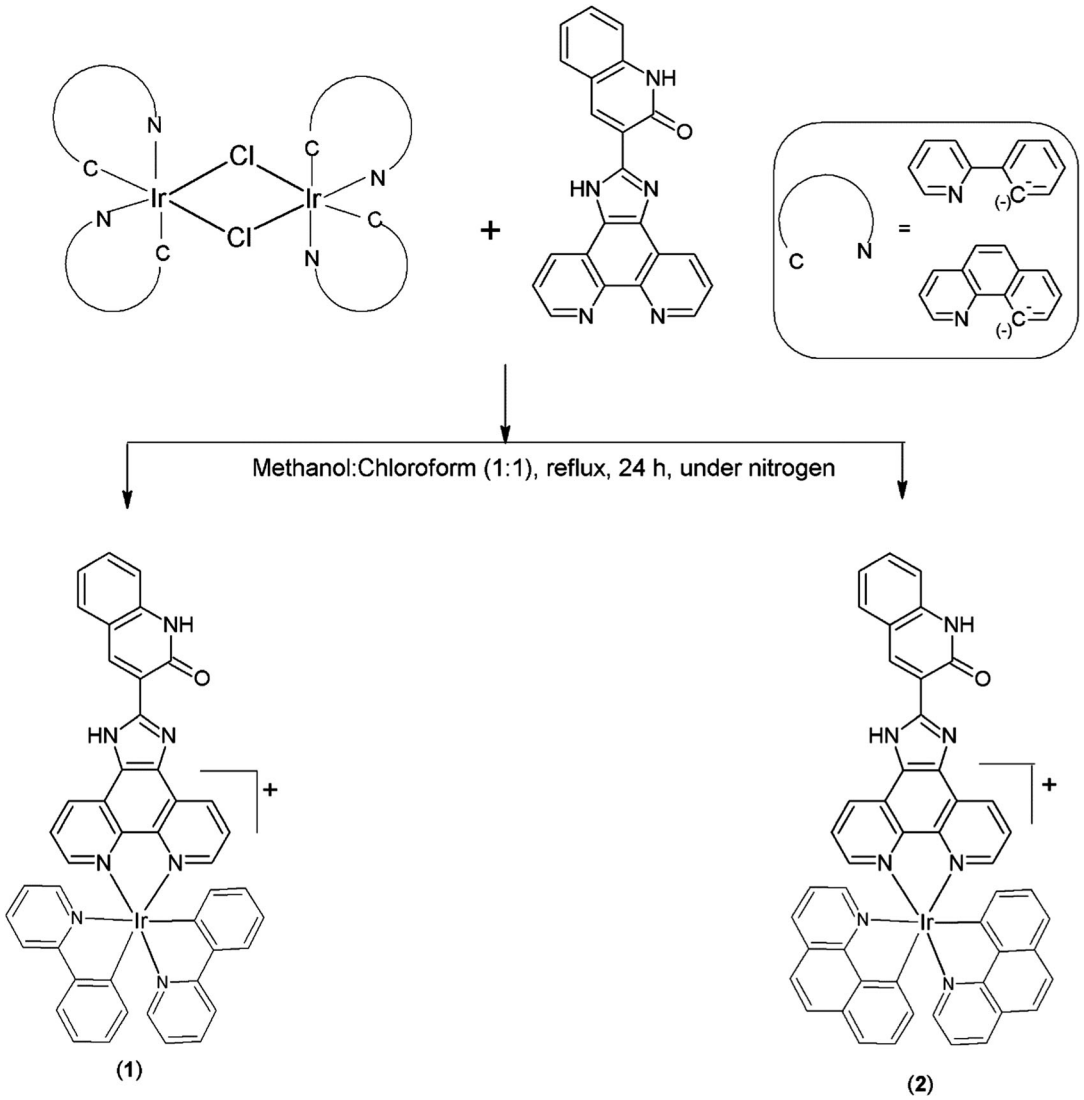

Scheme 1 The synthetic route for the synthesis of complexes **1** and **2**.

Due to the good chemical stability, medicinal properties and ease of synthetic modifications, quinoline derivatives represent an important class of compounds in drug and material chemistry.[41–43] Many biologically active compounds contains the quinoline moiety. A number of quinoline based compounds have antifungal, cardiotonic, antibacterial, antimalarial, anti-inflammatory, and antiprotozoic properties as well as antineoplastics acitivity.[41–44] Additionally, quinolines with high fluorescent quantum yields have been used as fluorescent probes in chemical sensors.[44–47]

As part of a program to develop metal-complex-based molecules targeting DNA binding properties, photophysical/imaging properties, and anticancer activity,[37,48–54] we have designed and synthesized quinoline-appended cyclometalated iridium(III) complexes $[Ir(ppy)_2(qip)]^+$ (**1**) and $[Ir(bhq)_2(qip)]^+$ (**2**) {ppy = 2-phenylpyridine, bhq = benzo[*h*]quinoline, Qip = 2(1*H*)-quinolinone-3(1*H*)-imidazo[4,5*f*][1,10]phenanthrolin-2-yl} (Scheme 1). Complexes containing different C–N ligands were synthesized to tune the lipophilicity and cellular uptake efficiency. The molecular structure of complex **2** is confirmed by single crystal X-ray crystallography. The photophysical properties of the complexes were investigated in different solvents and experimental results were compared with the theoretical results obtained from DFT and TD-DFT calculations. The interaction of the complexes with double stranded calf-thymus DNA (CT-DNA) was explored by spectroscopic techniques. The condensation of DNA by the complexes is studied by electrophoretic mobility studies. The cytotoxicity of the complexes against HeLa cell lines and subcellular localization of the complexes within the cells have been investigated.

Result and discussion

Synthesis and characterization

The ligand 2(1*H*)-quinolinone-3(1*H*)-imidazo[4,5*f*][1,10] phenanthrolin-2-yl (Qip) was synthesized by condensation of 1,10-phenanthroline-5,6-dione and 2-hydroxy-3-formyl-quinoline in

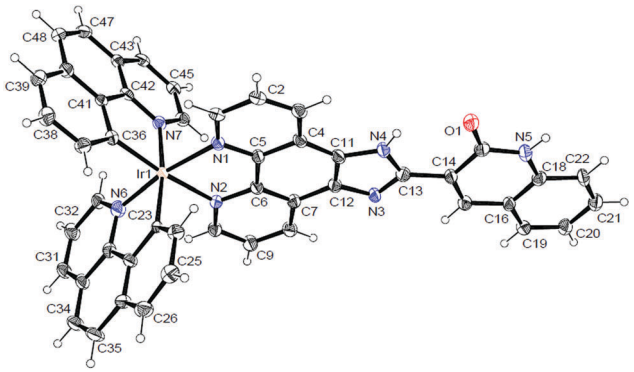

Fig. 1 ORTEP diagram of **2**, bond angles (°): N1–Ir1–N2 = 78.0(2); N7–Ir1–C36 = 81.0(2); N6–Ir1–C23 = 81.1(2): bond lengths (Å): Ir1– N1 = 2.145(5), Ir1–N2 = 2.107(6), Ir1–N6 = 2.031(6), Ir1–C23 = 2.075(6), Ir1–N7 = 2.057(5), Ir1–C36 = 2.021(6).

the presence of ammonium acetate in glacial acetic acid. The purified ligand is characterized by IR spectroscopy, ESI-MS, ^{1}H-NMR, and ^{13}C-NMR (see the Experimental section).

The iridium(III) complexes **1** and **2** were synthesized by refluxing Qip with an appropriate mole ratio of the precursor complex $[Ir(C–N)_2Cl]_2$ (C–N = ppy, bhq) in a chloroform and methanol mixture (Scheme 1). The complexes **1** and **2** were purified by neutral alumina column chromatography and characterized by ESI-MS, ^{1}H and ^{13}C NMR, IR and elemental analysis.

Single crystal structure of complex 2

Single crystals of complex **2** were obtained by vapor diffusion of diethyl ether into the solution of the perchlorate salt of the complex in dimethylformamide. Complex **2** crystallized in a triclinic crystal system with the $P\bar{1}$ space group. The Oak Ridge Thermal-Ellipsoid Plot (ORTEP) plot of complex **2** is given in Fig. 1 along with important bond lengths and angles. The single crystal structure refinement parameters for complex **2** are compiled in Table 1. The iridium atom within complex **2** had octahedral distortions, with an average bite angle between two bidentate carbene ligands of 81.0(2)° and polypyridine ligands of 78.0(2)°, which are similar to those reported for

Table 1 Crystal data and structure refinement parameters for complex **2**

Chemical formula	$2(C_{48}H_{29}IrN_7O)\cdot2(ClO_4)\cdot5(C_3H_7NO)\cdot(H_2O)$
M_r	2406.35
Crystal system, space group	Triclinic, $P\bar{1}$
a, b, c (Å)	15.9765(7), 19.1257(8), 19.7837(9)
α, β, γ (°)	107.484(2), 113.614(2), 95.893(2)
V (Å^3)	5108.1(4)
Z	2
Radiation type	Cu Kα
μ (mm^{-1})	6.09
Diffractometer	Bruker X8 Proteum
Absorption correction	Multi-scan SADABS
R_{int}	74 726, 16 741, 14 835
$(\sin q/l)_{max}$ (Å^{-1})	0.059
$R[F^2 > 2s(F^2)]$, $wR(F^2)$, S	0.051, 0.148, 1.04
No. of reflections	16 741
No. of parameters	1364
H-atom treatment	H-atom parameters constrained
ρ_{max}, $D\rho_{min}$ (e Å^{-3})	2.39, −0.93

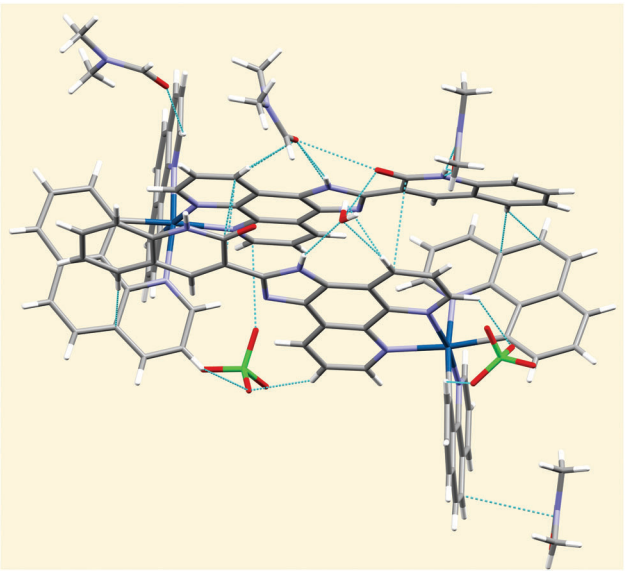

Fig. 2 Packing diagram of complex **2** showing the dimer formed by intermolecular hydrogen bonding involving cations and solvent molecules.

similar type complexes.[37] Complex **2** gets stabilized *via* intermolecular hydrogen bonding involving solvent molecules and cations leading to ''dimer'' formation (Fig. 2).

Photophysical properties

The UV-visible spectra of iridium complexes **1** and **2** recorded in dichloromethane at room temperature are given in Fig. 3a. Both the complexes showed intense intraligand (IL) transitions ($\pi \rightarrow \pi^*$) at approximately 220–350 nm. The less intense absorption shoulder at 350–420 nm is assigned to the spin allowed metal to ligand transitions (MLCT) by similarities with other reported systems.[37,55]

On excitation at 370 nm, complexes **1** and **2** emit green-orange fluorescence centered around 560 nm (Fig. 3b). The solution state emission by complexes **1** and **2** arises from ^{3}MLCT ($d\pi(Ir) \rightarrow \pi^*$) excited states.[26] In dichloromethane complexes **1** and **2** have a quantum yield of 0.126 and 0.134 respectively at room temperature (Table 2). Both the complexes have a lower emission quantum yield in a more polar solvent such as acetonitrile than the less polar CH_2Cl_2 solvent, which is similar to the observations reported for the cyclometalated iridium(III) MLCT emitting complexes.[26,56–67] The lower quantum yield of the complexes in a more polar solvent such as acetonitrile is due to the hydrogen-bonding interaction between the N–H groups of the diamine ligand and protic solvent molecules.[26]

Electronic structure calculations

Density Functional Theory (DFT) and Time-Dependent Density Functional Theory (TD-DFT) calculations of complexes **1** and **2** were studied in the dichloromethane solvent. The optimized structures of complexes **1** and **2** in the ground state (Fig. S5, ESI†) agree well with the single crystal X-ray data. Selected MOs of complexes **1** and **2** are given in Fig. 4 and Fig. S6 and orbital contributions are given in Table S2 (ESI†). The energy level diagram

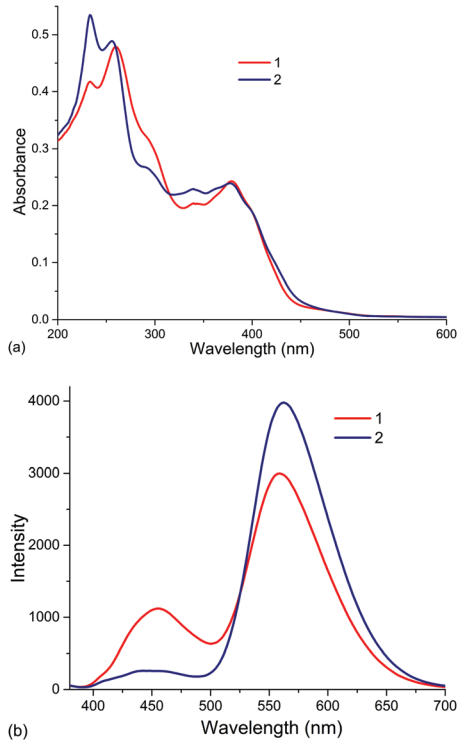

Fig. 3 (a) Absorption and (b) emission spectra of complexes **1** and **2** in dichloromethane (10 μM).

Table 2 Photo-physical properties of complexes **1** and **2**

		Emission			
		λ_{em} [b]	ϕ_{em} [c]	λ_{em} [b]	ϕ_{em} [c]
Complex[a]	Absorbance $\lambda_{max}/\varepsilon$ (M^{-1} cm^{-1}) (Dichloromethane) transitions	(Dichloromethane)		(Acetonitrile)	
1	233/42 000, 259/47 700 296/31 200, 339/20 600 379/24 300	558	0.126	466	0.029
2	232/56 500, 255/49 100 292/26 700, 338/23 000 378/23 700	563	0.134	562	0.006

[a] [Ir] = 10 (±0.2) μM. [b] Emission maxima. [c] ϕ = emission quantum yield excited at 370 nm, error limit: λ_{max} = ±2 nm, λ_{em} = ±2 nm, ϕ = ±5%. Relative quantum yield compared to $[Ru(bpy)_3]^{2+}$ ϕ = 0.028 in aerated aqueous solution.[41] The quantum yield values are corrected for the refractive index of the solvent according to ref. 40.

of molecular orbitals of complexes **1** and **2** is given in Fig. 5. The HOMO is localized on the iridium atom with some contribution from C–N ligands, while the HOMO−1 is mainly centered on the N–N polypyridyl ligand. The LUMO, LUMO+1, and LUMO+2 are located on the N–N polypyridyl ligand. The LUMO is mainly localized on the proximal position of the N–N donor polypyridyl ligand, while the LUMO+1 is localized on the distal portion of the ligand.

The electronic spectra of complexes **1** and **2** (Fig. 6) simulated by TD-DFT agree relatively well with the experimental results. The observed low energy band at 375 nm for complex **1** originates from HOMO−1 → LUMO+1 (67.9%), HOMO−2 → LUMO (21%), and HOMO → LUMO+4 (3.27%) and the observed low energy

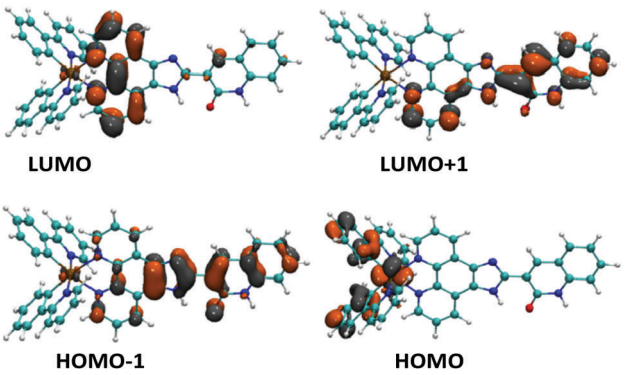

Fig. 4 Representations of HOMOs and LUMOs of complex **1**.

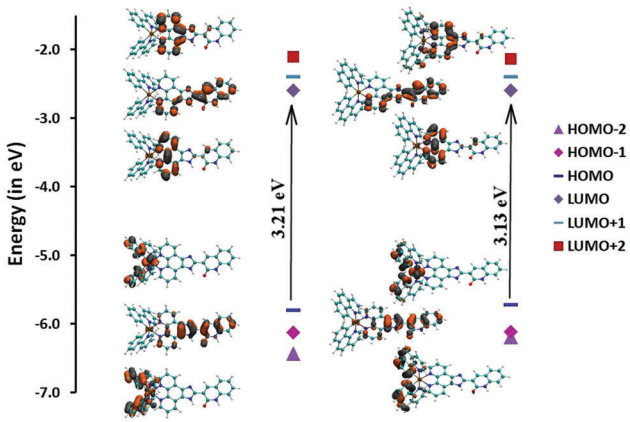

Fig. 5 The energy of the orbitals (in eV) for complexes **1–2** relative to the HOMO of the respective molecules.

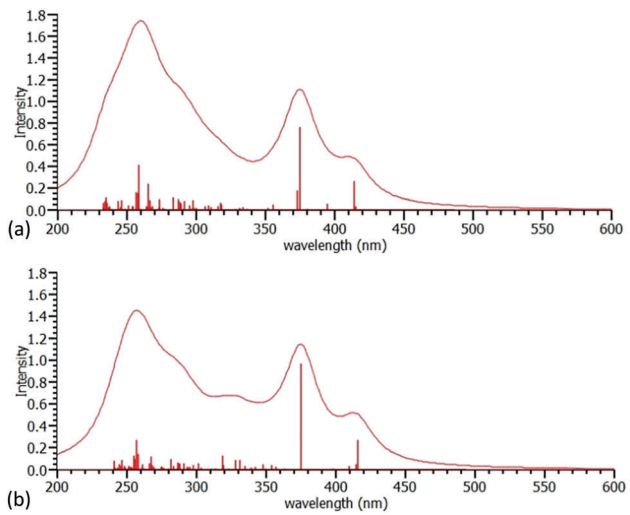

Fig. 6 TD-DFT calculated absorption spectra of complexes (a) **1** and (b) **2**.

band at 375 nm for complex **2** corresponds HOMO−1 → LUMO+1 (89.2%), and HOMO−2 → LUMO+1 (3.79%).

Biological properties

Before biological studies, the integrity of the complexes in water was investigated by UV-vis spectroscopy. The UV-visible

spectra of complexes recorded in water (containing 5% DMF) after dissolving immediately and after 24 h of dissolving did not show any significant changes confirming the stability of the complexes in water.

UV-Visible spectral titration

The UV-visible titration experiment is one of the widely used methodologies to study the interaction of synthetic molecules with DNA.[48–54,68–71] Iridium complexes **1** and **2** exhibited hypochromism upon addition of double-stranded calf thymus DNA (CT-DNA). The absorption spectra of complexes **1** and **2** upon addition of CT-DNA are shown in Fig. 7. Hypochromism of 40% and 16% was observed for complex **1** and **2** respectively at 380 nm indicating strong interaction of the complexes with CT-DNA.

The data obtained from the UV-visible titration experiments have been fitted with eqn (2) (Experimental section of ESI†) to estimate the intrinsic binding constants of complexes **1** and **2**. The intrinsic binding constants of complexes **1** and **2** were determined to be 3.92×10^4 M^{-1} and 1.52×10^4 M^{-1} (error limit ±5%) respectively. Lower binding constants suggest partial intercalation binding modes of complexes. The DNA binding constants of complexes **1** and **2** are comparable to that of the $[Ir(ppy)_2(dppz)]^+$ complex ($K_b = 2.0 \times 10^4$ M^{-1}),[26] but smaller than that of the well-known DNA intercalator $[Ru(bpy)_2(dppz)]^{2+}$ complex ($K_b = 4.0 \times 10^6$ M^{-1}).[72] The lower binding constants of the complexes used in the present study compared to the $[Ru(bpy)_2(dppz)]^{2+}$ complex may be due to the lower cationic charge of complexes **1** and **2**.

Emission titration studies

Further, the DNA binding properties of complexes **1** and **2** have been confirmed by emission titration experiments. The spectral changes in the emission spectra of complexes **1** and **2** upon addition of CT-DNA are shown in Fig. 8. The emission enhancement upon addition of CT-DNA was ascribed to the partial intercalation binding mode of iridium complexes **1** and **2** with CT-DNA. At higher concentrations of complex and CT-DNA the DNA condensates start precipitating as yellow threads. The fluorescence microscopy images of CT-DNA condensates are given in Fig. S7 (ESI†).

Electrophoretic mobility shift assay

Further, the interaction of complexes with plasmid pBr322 DNA was studied by electrophoretic mobility shift assay.[48,49] In the presence of complexes **1** and **2** DNA cleavage was not observed but retention of the DNA in the loading wells was observed (Fig. 9). The retention of DNA in the loading wells is due to the aggregation or condensation of DNA in the presence of complexes.[37,51,52] At higher concentration of complexes, complete condensation of DNA was observed. The condensation of DNA in the presence of complexes may be due to the intermolecular π···π contacts in the DNA-bound complexes, which lead to the collapse of part of DNA strands and initiate nucleation points for DNA condensation as observed in some of the reported ruthenium complexes.[73] DNA condensation is one of the major requirements to transport therapeutic genes into the

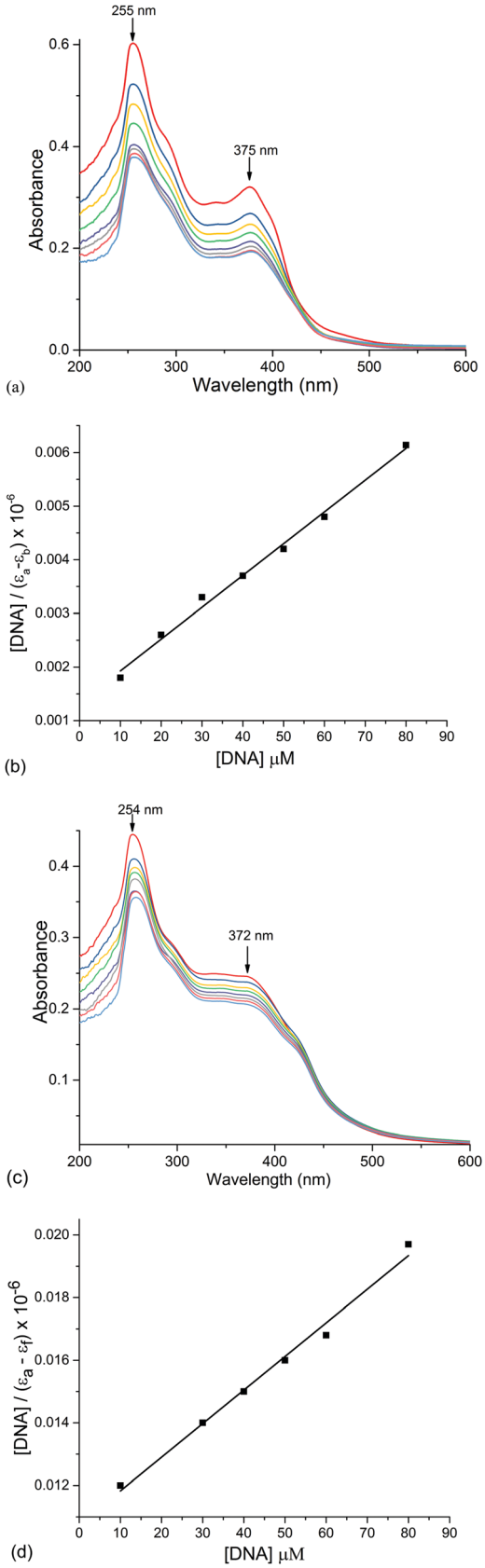

Fig. 7 Changes in the absorption spectra of complexes with increasing concentrations of CT-DNA (0–80 μM) (0.2 M phosphate buffer, pH 7.2) (a) **1** (10 μM), and (c) **2** (10 μM); (b and d) fitting of absorption data at 375 nm of complexes used to obtain the binding constants of complexes **1** and **2** respectively.

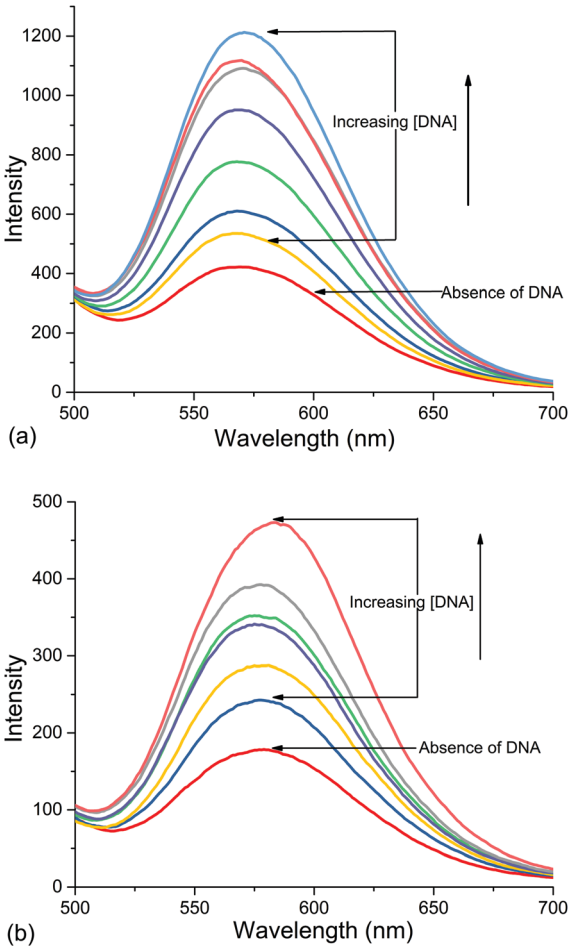

Fig. 8 Emission spectra of complexes (a) **1** (10 μM), and (b) **2** (10 μM) with increasing [CT-DNA]/[complex] ratio (0–20) in 0.2 M phosphate buffer, pH 7.2.

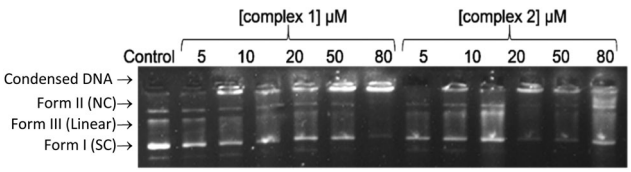

Fig. 9 Agarose gel (1%) electrophoresis of pBR322 DNA, [complex] = 5–80 μM, [DNA] = 200 ng, incubation 30 min at 37 °C, TBE buffer (40 mM Tris-acetate, 1 mM EDTA). Percentage of DNA band in control lane: NC 12.7%; linear 15.8; SC 68.1.

host cells to replace defective genes in the gene therapy process.[37,48,49,74,75]

Cytotoxicity studies

The cytotoxicity of cyclometalated complexes **1** and **2** towards HeLa cells was examined by MTT assay. The dose-dependent cytotoxicity of the complexes towards HeLa cells after treatment of 48 h is shown in Fig. 10. The IC_{50} values of complexes **1** and **2** are 60 μg mL^{-1}, which are on the same order of magnitude as the other reported iridium complexes. At a lower concentration range from 10–30 μM, these complexes exhibit low toxicity and can be further studied for their cellular imaging properties.

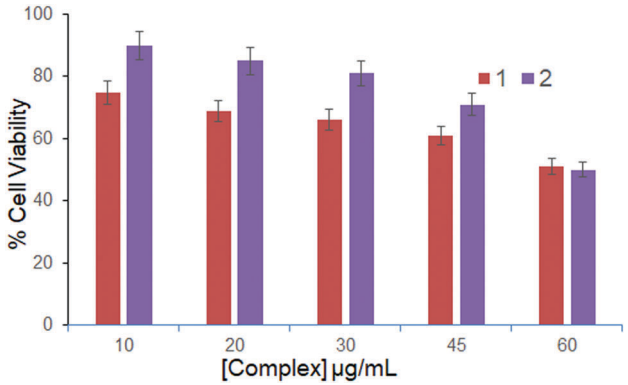

Fig. 10 Cytotoxicity evaluation of complexes **1** and **2** against the HeLa cell line. The cell viability was measured after 48 h by MTT assay, each data point represents the mean of three separate experiments.

Cellular uptake studies

Both the complexes are luminescent and exhibit low toxicity at the lower concentration range, so their cellular imaging ability was evaluated by fluorescence microscopy. For fluorescence microscopy studies HeLa cells were incubated with 10 μM of complexes for 1 h and then viewed under high resolution fluorescence microscopy; both the complexes accumulated throughout the cells (Fig. 11). Even localization of the complexes was observed throughout the cells without giving any preference to the nucleus.

Conclusions

In summary, two mononuclear iridium(III) complexes containing quinoline-appended ligands have been synthesized and characterized. Complex **2** has been characterized by single crystal X-ray structure determination. As per DFT calculations, the HOMO is localized mainly on iridium centers with some contribution from CN ligands and the LUMO is localized on the NN donor polypyridyl ligand in both the complexes. These complexes strongly interact with CT-DNA having a binding constant of the order of 10^4 M^{-1}. Both the complexes are less toxic to HeLa cells at lower concentrations. Further, fluorescence microscopy studies show that these complexes accumulate throughout the cell. These complexes have low toxicity and their strong intracellular luminescence highlights their potential as theragnostic agents.

Experimental section

Synthesis

1,10-Phenanthroline-5,6-dione[76] was synthesized according to the literature. The iridium precursor complexes $[Ir(ppy)_2Cl]_2$ and $[Ir(bhq)_2Cl]_2$ were prepared according to the reported procedure.[77]

2(1*H*)-Quinolinone-3(1*H*)-imidazo[4,5*f*][1,10]phenanthrolin-2-yl (Qip)

1,10-Phenanthroline-5,6-dione (0.60 g, 2.85 mmol), 2-hydroxy-3-formyl-quinoline (0.494 g, 2.85 mmol) and ammonium acetate

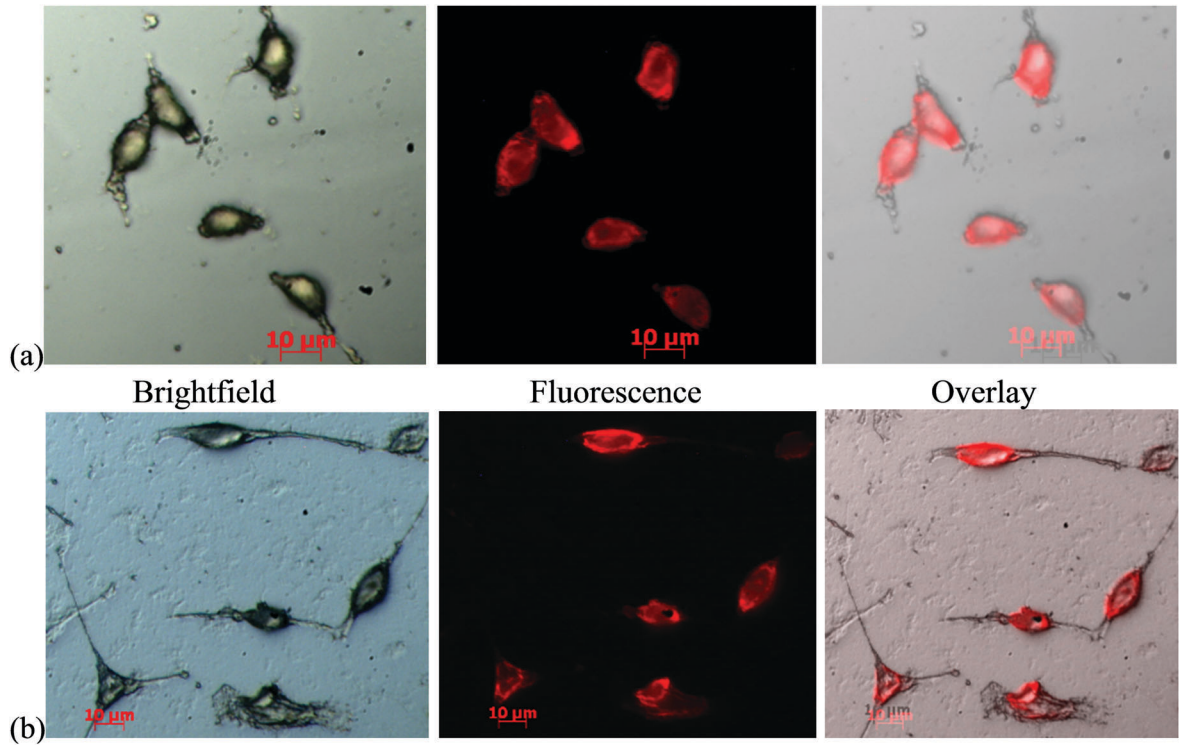

Fig. 11 High resolution fluorescence microscopy images of HeLa cells incubated (1 h) with 10 μM of (a) complex **1** (b) complex **2**.

(2.20 g, 28.5 mmol) were added to glacial acetic acid (20 mL) and refluxed for 6 h. The solution was cooled to room temperature and neutralized by liquid ammonia. The yellow precipitate formed was filtered and washed with water. The crude product obtained was purified by recrystallisation in methanol. Yield: 0.72 g (69%) ^{1}H NMR (DMSO-d_6, 400 MHz, 30 °C) δ = 7.30 (t, 1H), 7.47 (d, 1H),7.62 (t, 1H), 7.81 (m, 2H), 7.99 (d, 1H), 9.03 (dd, 3H), 9.10 (d, 2H); IR (cm^{-1}) 2922, 1716, 1651, 1601, 1578, 1477, 1213 ESI-MS: (*m*/*z*), (%) positive mode: 364 ([M + H]$^+$); anal. calcd for $C_{22}H_{13}N_5O$; C, 72.72; H 3.61; N 19.27 found: C, 72.61; H 3.54; N 19.17.

[Ir(ppy)$_2$(qip)]Cl (1)

A suspension of precursor complex $[Ir(ppy)_2Cl]_2$ (150 mg, 0.139 mmol) and Qip (101 mg, 0.278 mmol) in 40 mL methanol: chloroform (40 mL) was refluxed for 24 h under a nitrogen atmosphere in the dark. The reaction mixture was cooled and evaporated to dryness. The crude product obtained was purified by column chromatography on neutral alumina using acetonitrile : methanol (3 : 1). The orange yellow band was collected and evaporated to get the pure compound. Yield: 180 mg (71%) ^{1}H NMR (DMSO-d_6, 400 MHz, 30 °C) δ = 6.27 (d, 2H), 6.91 (m, 2H), 6.99 (m, 4H), 7.17 (m, 3H), 7.44 (m, 2H), 7.51 (d, 2H), 7.82 (m, 3H), 7.94 (m, 4H), 8.09 (t, 2H), 8.23 (d, 2H), 8.93 (s, 1H), 9.22 (d, 2H); ^{13}C NMR (DMSO-d_6, 100 MHz, 30 °C) δ = 120.40, 120.51, 122.88, 123.20, 124.37, 125.60, 127.28, 130.77, 131.75, 132.06, 133.12, 139.21, 139.75, 144.56, 144.63, 148.67, 149.68, 150.48, 151.02, 160.90, 167.44; IR (cm^{-1}): 3434, 3049, 2922, 1742, 1657, 1607, 1580, 1478, 1218, 785; ESI-MS: (*m*/*z*, (%) positive mode): 864.2 (100%) ([M − Cl]$^+$); anal. calcd for $C_{44}H_{29}N_7ClOIr$; C, 58.76; H 3.25; N 10.90 found: C, 58.64; H 3.17; N 10.63.

[Ir(bhq)$_2$(qip)]Cl (2)

The synthesis and purification of **2** was similar to that of **1** using $[Ir(bhq)_2Cl]_2$ (100 mg, 0.085 mmol) and Qip (62 mg, 0.17 mmol). Yield: 102 mg (63%). ^{1}H NMR (DMSO-d_6, 400 MHz, 30 °C) δ = 6.27 (d, 2H), 7.19 (m, 4H), 7.41 (m, 4H), 7.52 (t, 4H), 7.81–7.96 ~ (m, 10H), 8.08 (m, 2H), 8.48 (d, 2H), 9.03 (s, 1H); ^{13}C NMR (DMSO-d_6, 100 MHz, 30 °C) δ = 115.92, 119.49, 120.90, 123.31, 124.77, 127.22, 129.05, 129.69, 130.02, 130.27, 134.26, 138.09, 139.41, 140.86, 149.41, 149.70, 156.91, 160.85; IR (cm^{-1}): 3455, 3053, 2925, 1711, 1653, 1605, 1585, 1503, 1419, 1365, 1217, 1113, 783; ESI-MS: (*m*/*z*, (%) positive mode): 912.2 (100%) ([M − Cl]$^+$); anal. calcd for $C_{48}H_{29}N_7ClOIr$; C, 60.85; H 3.08; N 10.35 found: C, 60.74; H 3.01; N 10.03.

Methods and instrumentation

Details of methods/bio-assays used and instruments used in the present study are given in the ESI.†

Conflicts of interest

There are no conflicts to declare.

Acknowledgements

S. S. Bhat acknowledges the Science and Engineering Research Board, Department of Science and Technology, New Delhi,

India for financial support under the Start-Up-Grant (Young Scientist) project in Chemical Science (File no. YSS/2014/000546). RVP is grateful to the BRAF, C-DAC, Pune for providing the computational facility. SSB thanks Mr Pavan Bennur, USIC, Karnatak University, Dharwad for his kind help in recording high resolution fluorescence microscopy images. We thank SAIF Karnatak University Dharwad for NMR data, IIT Kanpur for ESI-MS data, and USIC, Karnatak University, Dharwad for providing instrumental facilities and Institute of excellence, University of Mysore, India for providing single crystal X-ray data.

References

1 C. Orvig and M. J. Abrams, *Chem. Rev.*, 1999, **99**, 2201–2204.
2 T. W. Hambley, *Dalton Trans.*, 2007, 4929–4937, DOI: 10.1039/b706075k.
3 C. Liu, M. Wang, T. Zhang and H. Sun, *Coord. Chem. Rev.*, 2004, **248**, 147–168.
4 J. Steinreiber and T. R. Ward, *Coord. Chem. Rev.*, 2008, **252**, 751–766.
5 Q. Jiang, N. Xiao, P. Shi, Y. Zhu and Z. Guo, *Coord. Chem. Rev.*, 2007, **251**, 1951–1972.
6 Y. Jung and S. J. Lippard, *Chem. Rev.*, 2007, **107**, 1387–1407.
7 E. R. Jamieson and S. J. Lippard, *Chem. Rev.*, 1999, **99**, 2467–2498.
8 E. Wong and C. M. Giandomenico, *Chem. Rev.*, 1999, **99**, 2451–2466.
9 T. Boulikas and M. Vougiouka, *Oncol. Rep.*, 2003, **10**, 1663–1682.
10 K. E. Erkkila, D. T. Odom and J. K. Barton, *Chem. Rev.*, 1999, **99**, 2777–2796.
11 M. R. Gill and J. A. Thomas, *Chem. Soc. Rev.*, 2012, **41**, 3179–3192.
12 B. M. Zeglis, V. C. Pierre and J. K. Barton, *Chem. Commun.*, 2007, 4565–4579, DOI: 10.1039/B710949K.
13 C. Metcalfe and J. A. Thomas, *Chem. Soc. Rev.*, 2003, **32**, 215–224.
14 R. Gao, D. G. Ho, B. Hernandez, M. Selke, D. Murphy, P. I. Djurovich and M. E. Thompson, *J. Am. Chem. Soc.*, 2002, **124**, 14828–14829.
15 L. Mosca, R. S. Khnayzer, M. S. Lazorski, E. O. Danilov, F. N. Castellano and P. Anzenbacher, *Chem. – Eur. J.*, 2015, **21**, 4056–4064.
16 M. C. DeRosa, D. J. Hodgson, G. D. Enright, B. Dawson, C. E. B. Evans and R. J. Crutchley, *J. Am. Chem. Soc.*, 2004, **126**, 7619–7626.
17 L. H. Fischer, M. I. J. Stich, O. S. Wolfbeis, N. Tian, E. Holder and M. Schäferling, *Chem. – Eur. J.*, 2009, **15**, 10857–10863.
18 Q. Zhao, F. Li, S. Liu, M. Yu, Z. Liu, T. Yi and C. Huang, *Inorg. Chem.*, 2008, **47**, 9256–9264.
19 E. Baranoff, J.-H. Yum, M. Graetzel and M. K. Nazeeruddin, *J. Organomet. Chem.*, 2009, **694**, 2661–2670.
20 C. Ulbricht, B. Beyer, C. Friebe, A. Winter and U. S. Schubert, *Adv. Mater.*, 2009, **21**, 4418–4441.
21 L. Xiao, Z. Chen, B. Qu, J. Luo, S. Kong, Q. Gong and J. Kido, *Adv. Mater.*, 2011, **23**, 926–952.
22 N. Rehmann, C. Ulbricht, A. Köhnen, P. Zacharias, M. C. Gather, D. Hertel, E. Holder, K. Meerholz and U. S. Schubert, *Adv. Mater.*, 2008, **20**, 129–133.
23 N. Tian, A. Thiessen, R. Schiewek, O. J. Schmitz, D. Hertel, K. Meerholz and E. Holder, *J. Org. Chem.*, 2009, **74**, 2718–2725.
24 B. Ma, F. Lauterwasser, L. Deng, C. S. Zonte, B. J. Kim, J. M. J. Fréchet, C. Borek and M. E. Thompson, *Chem. Mater.*, 2007, **19**, 4827–4832.
25 E. Holder, B. M. W. Langeveld and U. S. Schubert, *Adv. Mater.*, 2005, **17**, 1109–1121.
26 K. K.-W. Lo, C.-K. Chung and N. Zhu, *Chem. – Eur. J.*, 2006, **12**, 1500–1512.
27 Q. Zhao, M. Yu, L. Shi, S. Liu, C. Li, M. Shi, Z. Zhou, C. Huang and F. Li, *Organometallics*, 2010, **29**, 1085–1091.
28 K. K.-W. Lo, K. Y. Zhang, S.-K. Leung and M.-C. Tang, *Angew. Chem., Int. Ed.*, 2008, **47**, 2213–2216.
29 K.-H. Leung, H.-Z. He, B. He, H.-J. Zhong, S. Lin, Y.-T. Wang, D.-L. Ma and C.-H. Leung, *Chem. Sci.*, 2015, **6**, 2166–2171.
30 S. Liu, H. Liang, K. Y. Zhang, Q. Zhao, X. Zhou, W. Xu and W. Huang, *Chem. Commun.*, 2015, **51**, 7943–7946.
31 L. He, Y. Li, C.-P. Tan, R.-R. Ye, M.-H. Chen, J.-J. Cao, L.-N. Ji and Z.-W. Mao, *Chem. Sci.*, 2015, **6**, 5409–5418.
32 R.-R. Ye, C.-P. Tan, L.-N. Ji and Z.-W. Mao, *Dalton Trans.*, 2016, **45**, 13042–13051.
33 K. Qiu, Y. Liu, H. Huang, C. Liu, H. Zhu, Y. Chen, L. Ji and H. Chao, *Dalton Trans.*, 2016, **45**, 16144–16147.
34 Y. Hisamatsu, N. Suzuki, A.-A. Masum, A. Shibuya, R. Abe, A. Sato, S.-I. Tanuma and S. Aoki, *Bioconjugate Chem.*, 2017, **28**, 507–523.
35 J. M. Fernández-Hernández, C.-H. Yang, J. I. Beltrán, V. Lemaur, F. Polo, R. Fröhlich, J. Cornil and L. D. Cola, *J. Am. Chem. Soc.*, 2011, **133**, 10543–10558.
36 S. Mukhopadhyay, R. S. Singh, R. P. Paitandi, G. Sharma, B. Koch and D. S. Pandey, *Dalton Trans.*, 2017, **46**, 8572–8585.
37 S. S. Bhat, N. Shivalingegowda, V. K. Revankar, N. K. Lokanath, M. S. Kugaji, V. Kumbar and K. Bhat, *J. Inorg. Biochem.*, 2017, **177**, 127–137.
38 J. Liu, C. Jin, B. Yuan, X. Liu, Y. Chen, L. Ji and H. Chao, *Chem. Commun.*, 2017, **53**, 2052–2055.
39 D. P. Smith, H. Chen, S. Ogo, A. I. Elduque, M. Eisenstein, M. M. Olmstead and R. H. Fish, *Organometallics*, 2014, **33**, 2389–2404.
40 S. Mukhopadhyay, R. K. Gupta, R. P. Paitandi, N. K. Rana, G. Sharma, B. Koch, L. K. Rana, M. S. Hundal and D. S. Pandey, *Organometallics*, 2015, **34**, 4491–4506.
41 R. Musiol, J. Jampilek, K. Kralova, D. R. Richardson, D. Kalinowski, B. Podeszwa, J. Finster, H. Niedbala, A. Palka and J. Polanski, *Bioorg. Med. Chem.*, 2007, **15**, 1280–1288.
42 A. Marella, O. P. Tanwar, R. Saha, M. R. Ali, S. Srivastava, M. Akhter, M. Shaquiquzzaman and M. M. Alam, *Saudi Pharm. J.*, 2013, **21**, 1–12.
43 K. Kaur, M. Jain, R. P. Reddy and R. Jain, *Eur. J. Med. Chem.*, 2010, **45**, 3245–3264.
44 B. Czaplinska, A. Maron, J. G. Malecki, G. Szafraniec-Gorol, M. Matussek, K. Malarz, A. Mrozek-Wilczkiewicz,

W. Danikiewicz, R. Musiol and A. Slodek, *Dyes Pigm.*, 2017, **144**, 119–132.
45 N. Perin, M. Hranjec, G. Pavlović and G. Karminski-Zamola, *Dyes Pigm.*, 2011, **91**, 79–88.
46 C.-H. Tseng, Y.-R. Chen, C.-C. Tzeng, W. Liu, C.-K. Chou, C.-C. Chiu and Y.-L. Chen, *Eur. J. Med. Chem.*, 2016, **108**, 258–273.
47 R. Slavik, A. M. Herde, D. Bieri, M. Weber, R. Schibli, S. D. Krämer, S. M. Ametamey and L. Mu, *Eur. J. Med. Chem.*, 2015, **92**, 554–564.
48 S. S. Bhat, V. K. Revankar, A. Khan, R. V. Pinjari and M. Necas, *Chem. – Asian J.*, 2017, **12**, 254–264.
49 S. S. Bhat, V. K. Revankar, R. V. Pinjari, N. S, C. Bogar, K. Bhat and V. A. Kawade, *New J. Chem.*, 2017, **41**, 5513–5520.
50 S. S. Bhat, V. K. Revankar, A. Khan, R. J. Butcher and K. Thatipamula, *New J. Chem.*, 2015, **39**, 3646–3657.
51 S. S. Bhat, A. S. Kumbhar, A. A. Kumbhar and A. Khan, *Chem. – Eur. J.*, 2012, **18**, 16383–16392.
52 S. S. Bhat, A. S. Kumbhar, A. A. Kumbhar, A. Khan, P. Lonnecke and E. Hey-Hawkins, *Chem. Commun.*, 2011, **47**, 11068–11070.
53 S. S. Bhat, A. A. Kumbhar, H. Heptullah, A. A. Khan, V. V. Gobre, S. P. Gejji and V. G. Puranik, *Inorg. Chem.*, 2011, **50**, 545–558.
54 S. S. Bhat, A. S. Kumbhar, P. Lönnecke and E. Hey-Hawkins, *Inorg. Chem.*, 2010, **49**, 4843–4853.
55 C. Wang, L. Lystrom, H. Yin, M. Hetu, S. Kilina, S. A. McFarland and W. Sun, *Dalton Trans.*, 2016, **45**, 16366–16378.
56 G. Calogero, G. Giuffrida, S. Serroni, V. Ricevuto and S. Campagna, *Inorg. Chem.*, 1995, **34**, 541–545.
57 F. Neve, M. La Deda, A. Crispini, A. Bellusci, F. Puntoriero and S. Campagna, *Organometallics*, 2004, **23**, 5856–5863.
58 I. M. Dixon, J.-P. Collin, J.-P. Sauvage, L. Flamigni, S. Encinas and F. Barigelletti, *Chem. Soc. Rev.*, 2000, **29**, 385–391.
59 M. G. Colombo, A. Hauser and H. U. Güdel, in *Electronic and Vibronic Spectra of Transition Metal Complexes I*, ed. H. Yersin, Springer, Berlin, Heidelberg, 1994, pp. 143–171, DOI: 10.1007/3-540-58155-3_5.
60 M. G. Colombo, A. Hauser and H. U. Guedel, *Inorg. Chem.*, 1993, **32**, 3088–3092.
61 J. H. van Diemen, J. G. Haasnoot, R. Hage, E. Müller and J. Reedijk, *Inorg. Chim. Acta*, 1991, **181**, 245–251.
62 P. Coppo, E. A. Plummer and L. D. Cola, *Chem. Commun.*, 2004, 1774–1775, DOI: 10.1039/B406851C.
63 E. A. Plummer, J. W. Hofstraat and L. D. Cola, *Dalton Trans.*, 2003, 2080–2084, DOI: 10.1039/B300704A.
64 C. Schaffner-Hamann, A. von Zelewsky, A. Barbieri, F. Barigelletti, G. Muller, J. P. Riehl and A. Neels, *J. Am. Chem. Soc.*, 2004, **126**, 9339–9348.
65 F.-M. Hwang, H.-Y. Chen, P.-S. Chen, C.-S. Liu, Y. Chi, C.-F. Shu, F.-I. Wu, P.-T. Chou, S.-M. Peng and G.-H. Lee, *Inorg. Chem.*, 2005, **44**, 1344–1353.
66 K. K.-W. Lo, C.-K. Chung and N. Zhu, *Chem. – Eur. J.*, 2003, **9**, 475–483.
67 K. K.-W. Lo, D. C.-M. Ng and C.-K. Chung, *Organometallics*, 2001, **20**, 4999–5001.
68 S. Stimpson, D. R. Jenkinson, A. Sadler, M. Latham, D. A. Wragg, A. J. H. M. Meijer and J. A. Thomas, *Angew. Chem., Int. Ed.*, 2015, **54**, 3000–3003.
69 A. Ghosh, A. Mandoli, D. K. Kumar, N. S. Yadav, T. Ghosh, B. Jha, J. A. Thomas and A. Das, *Dalton Trans.*, 2009, 9312–9321, DOI: 10.1039/B906756F.
70 H. Xu, K.-C. Zheng, H. Deng, L.-J. Lin, Q.-L. Zhang and L.-N. Ji, *New J. Chem.*, 2003, **27**, 1255–1263.
71 P. P. Pellegrini and J. R. Aldrich-Wright, *Dalton Trans.*, 2003, 176–183, DOI: 10.1039/B208147D.
72 W. A. Kalsbeck and H. H. Thorp, *J. Am. Chem. Soc.*, 1993, **115**, 7146–7151.
73 B. Sun, J.-X. Guan, L. Xu, B.-L. Yu, L. Jiang, J.-F. Kou, L. Wang, X.-D. Ding, H. Chao and L.-N. Ji, *Inorg. Chem.*, 2009, **48**, 4637–4639.
74 Y. Liu, Z.-L. Yu, Y.-M. Zhang, D.-S. Guo and Y.-P. Liu, *J. Am. Chem. Soc.*, 2008, **130**, 10431–10439.
75 I. W. Hamley and V. Castelletto, *Angew. Chem., Int. Ed.*, 2007, **46**, 4442–4455.
76 Y. Masaki, T. Yoshihito, Y. Yasuyuki, K. Shigeyasu and S. Ichiro, *Bull. Chem. Soc. Jpn.*, 1992, **65**, 1006–1011.
77 N. Matsuo, *Bull. Chem. Soc. Jpn.*, 1974, **47**, 767–768.

